

Lightning Fast Video Anomaly Detection via Adversarial Knowledge Distillation

Nicolae-Cătălin Ristea^{1,2}, Florinel-Alin Croitoru¹, Dana Dăscălescu¹, Radu Tudor Ionescu^{1,3,*},
Fahad Shahbaz Khan^{4,5}, Mubarak Shah⁶

¹University of Bucharest, Romania, ²University Politehnica of Bucharest, Romania,

³SecurifAI, Romania, ⁴MBZ University of Artificial Intelligence, UAE,

⁵Linköping University, Sweden, ⁶University of Central Florida, US

Abstract

We propose a very fast frame-level model for anomaly detection in video, which learns to detect anomalies by distilling knowledge from multiple highly accurate object-level teacher models. To improve the fidelity of our student, we distill the low-resolution anomaly maps of the teachers by jointly applying standard and adversarial distillation, introducing an adversarial discriminator for each teacher to distinguish between target and generated anomaly maps. We conduct experiments on three benchmarks (Avenue, ShanghaiTech, UCSD Ped2), showing that our method is over 7 times faster than the fastest competing method, and between 28 and 62 times faster than object-centric models, while obtaining comparable results to recent methods. Our evaluation also indicates that our model achieves the best trade-off between speed and accuracy, due to its previously unheard-of speed of 1480 FPS. In addition, we carry out a comprehensive ablation study to justify our architectural design choices.

1. Introduction

Video anomaly detection is a difficult task, being actively studied in recent years [1–31] due to its increasing importance. The difficulty of the task stems from the fact that abnormal events depend on the context and occur rarely. To illustrate the scarcity and reliance on context of abnormal events, we consider the truck deliberately driven into the Berlin Christmas market¹ in 2016 as a relevant example. A truck driven on the road is labeled as a normal event, but, as soon as the truck intrudes into a pedestrian area, *e.g.* a market, the event becomes abnormal. This example confirms that labeling an event as normal or abnormal depends on the context. Moreover, according to Wikipedia², there are about 170 vehicle ramming attacks registered since 1953 to date, but many of them are too old to be caught on video. Hence, our example also confirms that such events rarely occur.

*corresponding author: raducu.ionescu@gmail.com

¹https://en.wikipedia.org/wiki/2016_Berlin_truck_attack

²https://en.wikipedia.org/wiki/Vehicle-ramming_attack

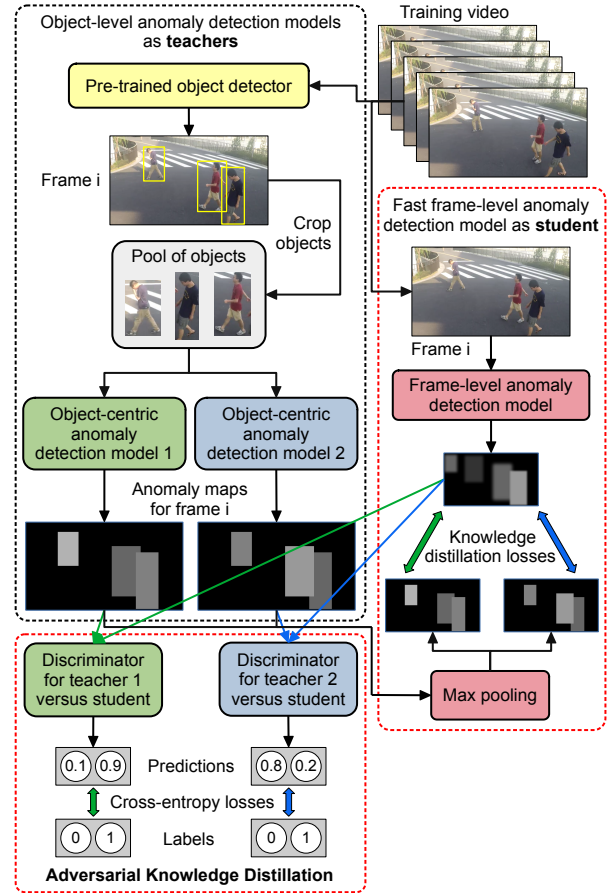


Figure 1. Our pipeline comprising an efficient student model that learns to distill knowledge from two object-centric teachers via a combination of direct and adversarial losses. The pipeline can be trivially extended to any number of teachers. For simplicity, we do not represent the multi-frame input and multi-resolution output of our student. Best viewed in color.

Due to the rarity and reliance on context of abnormal events, it is nearly impossible to collect a sufficiently representative set of such events, eliminating the possibility of applying traditional approaches based on supervised learning to perform video anomaly detection. With the supervised option thrown out the window, researchers turned their attention to alternative solutions, the most prominent alternative

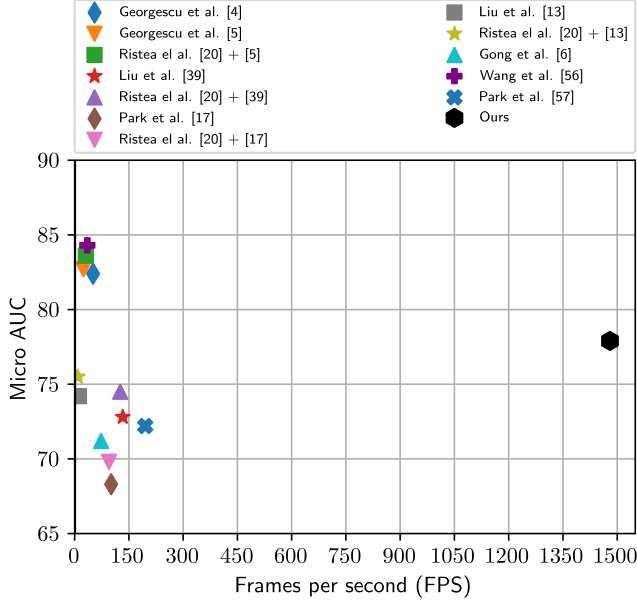


Figure 2. The trade-off between performance (micro AUC) and speed (FPS) for our student versus multiple state-of-the-art methods [4–6, 13, 17, 20, 39, 56, 57] (with open-sourced code), on the ShanghaiTech data set. The running times of all methods are measured on a machine with an Nvidia GeForce GTX 3090 GPU with 24 GB of VRAM. Best viewed in color.

being based on outlier detection [2, 8, 11, 17–19, 23, 26, 32–55]. Methods based on outlier detection learn a normality model from training videos containing only normal events, labeling test samples that deviate from the model as abnormal. Our approach falls within the same line of research, being based on distilling knowledge from object-centric outlier detection systems [4, 5], which reported state-of-the-art performance levels in anomaly detection. We hereby emphasize that top scoring abnormal event detection systems such as [4, 5, 7] operate at the object level, relying on a pre-trained object detector which limits the real-time processing to only a single video stream per GPU. Although it might seem sufficient to process one video stream at about 20–30 FPS on one GPU, the cost of computational resources to process tens or hundreds of video streams (as expected in real-world surveillance scenarios) quickly becomes very high, considering that the price range of one GPU is around \$1000–4000. The high cost of the computational resources adds to the difficulty of solving the video anomaly detection task in the real-world.

To address the aforementioned efficiency problem, we propose a fast anomaly detection model based on a novel convolutional transformer that replaces fully connected layers inside the transformer with pointwise convolutional layers. Our model operates at the frame level, eliminating the need for a pre-trained object detector. At the same time, we aim to reach an accuracy level that is as close as possible to that of object-centric models. To this end, we train our model in a teacher-student setup, learning to detect anomalies by distill-

ing knowledge from multiple highly accurate object-centric teacher models. Aside from the conventional distillation process based on the mean squared error between the low-resolution anomaly maps of the student and each teacher, we introduce an adversarial discriminator to distinguish between target (teacher) and reproduced (student) anomaly maps, as shown in Figure 1. To the best of our knowledge, we are the first to propose an adversarial knowledge distillation framework for anomaly detection in video.

We conduct experiments on three benchmark data sets: Avenue [40], ShanghaiTech [41] and UCSD Ped2 [42]. Our empirical evaluation shows that our method is between 28 to 62 times faster compared to object-centric models (1480 FPS versus 24–52 FPS), while obtaining performance levels that are comparable to many recent methods [3, 7, 8, 13, 17, 22, 23, 44, 58–61] and less than 5% below the object-centric teachers [4, 5]. As shown in Figure 2, our model achieves the best trade-off between speed and accuracy. In addition, we carry out a comprehensive ablation study to justify our architectural design choices. The ablation study is discussed in the supplementary.

In summary, our contribution is threefold:

- We propose a novel teacher-student framework for anomaly detection in video, learning to detect anomalies by distilling knowledge from multiple highly accurate object-level teachers into a highly efficient student.
- We propose adversarial knowledge distillation in the context of anomaly detection, introducing an adversarial discriminator for each teacher to distinguish between original (teacher) and reproduced (student) outputs.
- To increase the processing speed and reduce the number of learnable weights, we replace the fully connected layers inside the transformer blocks forming the student with pointwise convolutional layers.

2. Related Work

2.1. Video Anomaly Detection

Most frameworks formulate anomaly detection as a one-class learning problem, where only normal data is available at training time, while both normal and abnormal examples are present at test time [19, 62]. The anomaly detection approaches are typically categorized into dictionary learning methods [33–35, 40, 48], probabilistic models [32, 37, 42, 43, 63–67], distance-based approaches [7, 8, 18, 21, 44, 46, 49, 68–71], reconstruction-based methods [6, 15, 17, 20, 23, 36, 39, 41, 47, 72, 73] and change detection frameworks [9, 16, 74, 75]. From a different perspective, the anomaly detection methods can also be divided into frame-level [8, 21, 39, 40, 42, 43, 46, 47, 49, 53, 59, 69, 75] and object-level [3–5, 7, 27, 56, 58, 76] frameworks, according to the level at which the anomaly detection algorithm is applied. These two categories are extensively described below.

Frame-level methods. Frame-level methods detect anomalies by taking entire video frames as input. Yu *et al.* [59] proposed a frame-level framework that employs the adversarial learning of past and future events to detect anomalies. Liu *et al.* [39] proposed a simple yet effective algorithm, which learns to reconstruct the next frame of a short video sequence. A more complex approach is proposed by Liu *et al.* [13], which conditions the image prediction on optical flow reconstruction using a conditional Variational Auto-Encoder (VAE). Considering that frame-level methods commonly rely on producing poor reconstructions for anomalies, generalizing to out-of-distribution samples, *e.g.* anomalies, is not desired. To reduce the generalization capability, researchers employed various techniques, such as adding memory modules [6, 13, 17] or masked convolutional blocks [20]. Although integrating additional modules into the network leads to accuracy gains, the procedure often comes with a significant efficiency penalty. Focusing primarily on efficiency, we propose a novel adversarial distillation framework that teaches our efficient frame-level student to replicate two heavy object-level teachers [4, 5]. By distilling powerful teachers, we can afford to employ a lightweight frame-level student, gaining between 28 and 62 times the speed of the teachers with just a small performance drop (less than 5%).

Object-level methods. Lately, several powerful algorithms have been developed for anomaly detection by estimating anomaly scores at the object level [4, 5, 7, 27, 56, 58], rather than at the frame level. Since the abnormal examples can be described as unusual objects in a regular scene, the prior information from an object detector enables anomaly detection models to focus only on objects, boosting the performance by a significant margin. One of the first object-level models is proposed in [7]. The method of Ionescu *et al.* [7] applies a k-means clustering in the joint latent space of motion and appearance auto-encoders. Georgescu *et al.* [5] extended the framework of [7] by introducing pseudo-anomalies during training and attaching classifiers to discriminate between normal and pseudo-abnormal samples.

Georgescu *et al.* [4] employed self-supervised multi-task learning at the object-level to detect anomalies in video. The framework uses a total of four proxy tasks, three based on self-supervision and one based on knowledge distillation. The final anomaly score for each object detected in a frame is computed by averaging the anomaly scores predicted for each proxy task. The approach is further developed in [58], leveraging additional proxy tasks and a transformer-based architecture. Wang *et al.* [56] studied alternative proxy tasks based on solving spatial and temporal jigsaw puzzles.

Most object-level methods rely on running an object detector, which limits the processing time to the speed of the detector. Thus, efficiency is significantly impacted, as the speed of the detector is often much lower than that of the anomaly detection network [4, 7]. To address this issue, we

propose a frame-level framework that is trained to reproduce the output of two strong object-level teachers [4, 5], eliminating the object detector from the equation during inference.

Methods addressing efficiency. While video anomaly detection has been extensively studied in recent years, the top scoring methods have certain speed limitations, preventing the deployment of state-of-the-art approaches in real-world scenarios, *e.g.* in video surveillance of entire cities. Even so, there is limited research on efficient anomaly detection frameworks [57, 77–79], and an acceptable trade-off between speed and performance has not been achieved yet. Doshi *et al.* [79] proposed a video anomaly detection system that is capable of running on roadside cameras, while Li *et al.* [77] proposed a neural architecture that learns normal behavior without supervision. In our work, we design a lightweight hybrid convolutional-transformer student network that is trained to mimic the output of highly complex and accurate teachers, in an adversarial fashion. The limited complexity of our student leads to processing more than 1480 frames per second (FPS), while achieving competitive accuracy. Compared to competing methods, we achieve a significantly better speed versus performance trade-off.

2.2. Transformers

Vaswani *et al.* [80] proposed a model based purely on self-attention, leading the way forward for research on neural architectures relying on attention, including vision transformers [81–92]. Transformers have been widely adopted in computer vision, due to the outstanding results across a broad variety of tasks, ranging from object recognition [83, 87, 88] and object detection [81, 91, 92] to image generation [86, 89, 90]. Distinct from approaches using only transformer-based attention [81–88, 91, 92], we propose a hybrid model, composed of both convolutional and self-attention blocks, to reduce the usually high processing time of transformers. More precisely, we improve the efficiency by downsampling the input and by replacing fully connected layers with pointwise convolutional layers.

To the best of our knowledge, there are only a handful of works applying transformers to video anomaly detection [58, 93–96]. Unlike these related methods, which barely discuss the efficiency problem, our work is the first to significantly improve the accuracy versus efficiency trade-off of transformers for anomaly detection.

2.3. Knowledge Distillation

As a strategy for compressing one or multiple highly complex models, knowledge distillation [97, 98] aims to efficiently train a lightweight neural network, called *student*, under the supervision of one or more deeper neural networks, called *teachers*, achieving competitive performance with fewer computational resources. Knowledge distillation, also known as teacher-student training, was recently adopted for various image classification tasks [99], *e.g.* ob-

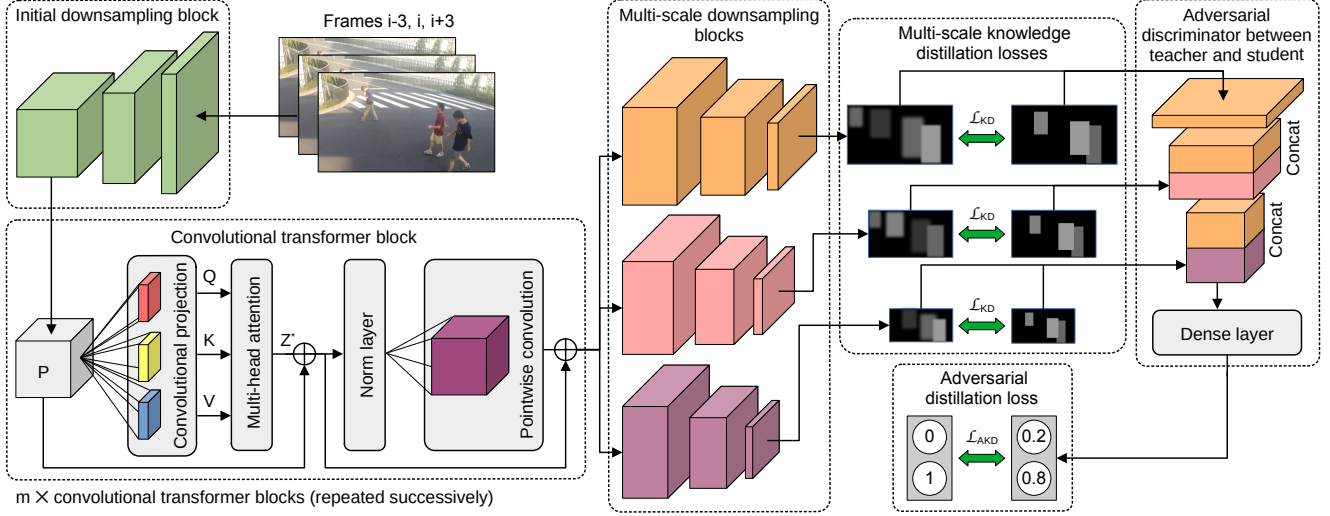


Figure 3. Architecture of our student based on a convolutional transformer and multiple downsampling blocks. For simplicity, we represent the adversarial discriminator and anomaly maps for only one teacher. Best viewed in color.

ject recognition [100–103], face recognition [104, 105] and anomaly detection [5, 106–110]. We next present closely related distillation methods applied to anomaly detection. Bergmann *et al.* [106] framed anomaly detection as a feature regression problem, training an ensemble of student models on anomaly-free data to replicate the output of a descriptive feature extractor, pre-trained on a large data set of natural images. The authors used the inherent uncertainty of the student networks as an anomaly scoring function. In a similar fashion, Salehi *et al.* [109] proposed to distill the features at different layers of a teacher pre-trained on ImageNet. A similar approach was proposed by Cheng *et al.* [107], which distills the flow of solution procedure (FSP) matrix from adjacent layers. A distinct approach was introduced in [108], in which the teacher-student framework consists of a student decoder that receives as input the one-class embedding produced by a teacher encoder. The above methods are mainly focused on knowledge distillation applied to image anomaly detection. Comparatively lower attention has been devoted to applying knowledge distillation to video anomaly detection. In [110], the authors employed a self-taught system based on a teacher-student model that does not require human-annotated data. Similarly, Georgescu *et al.* [5] employed knowledge distillation and integrated the paradigm with several self-supervised tasks.

The methods employing knowledge distillation for image or video anomaly detection leverage the representation discrepancy of anomalies between the teacher and the student models, which requires running both teacher and student models during inference. Unlike the aforementioned methods, we perform knowledge distillation from teachers designed for video anomaly detection, specifically aiming to improve the computational time, running only the student model at test time. Moreover, to the best of our knowledge,

we are the first to introduce adversarial knowledge distillation in the context of anomaly detection.

3. Method

Overview. We next provide an overview of our approach for training a fast and competitive frame-level model for video anomaly detection. The training process is divided into two phases. In the first training phase, we attach a decoder to our network and train it as an auto-encoder to reconstruct normal training data, in a similar manner to [11, 39]. Afterwards, we discard the decoder, attach three anomaly detection heads to the model and train it via knowledge distillation. We employ two strategies to distill the knowledge from two object-level anomaly detection teacher models [4, 5] into our student, as illustrated in Figure 1. The first strategy is based on minimizing the mean squared error between the target anomaly maps provided by the teachers and the anomaly maps predicted by the student. The second strategy is based on adversarial training, relying on a neural discriminator that is optimized to distinguish between student and teacher anomaly maps. At the same time, our student is trained with an adversarial loss, trying to fool the discriminator. In this training setting, the student becomes a conditional generator. We next present the architecture and the training procedure of our network.

Student architecture. As depicted in Figure 3, the architecture of our student network starts with a downsampling block which reduces the spatial dimensions of the input frames, while increasing the number of feature maps. The second part of the architecture is formed of m adapted convolution vision transformer (CvT) [88] blocks. The adaptation consists of replacing all fully connected layers with pointwise convolutional layers to speed up the computation. The last part incorporates three multi-scale downsampling blocks

generating anomaly maps at various resolutions.

The downsampling block includes five convolutional layers, each followed by a batch normalization layer and Rectified Linear Units (ReLU) [111]. The first convolutional layer is formed of 16 filters with a spatial size of 7×7 and no padding. The subsequent convolutional layers of the downsampling block have 32, 64, 128 and 256 filters, respectively, each with a kernel size of 3×3 . Each layer uses a stride of 2 and a padding of 1.

Let $P \in \mathbb{R}^{h \times w \times c}$ denote the output tensor of the downsampling block, where h , w and c represent the height, the width and the number of channels. P is further processed by a convolutional transformer. The transformer encloses m consecutive transformer blocks and interprets P as a set of overlapping visual tokens. The transformer blocks follow the implementation of Wu *et al.* [88], where, prior to the self-attention mechanism, the queries Q , the keys K and the values V are computed from P via convolutional projection. This operation is a depthwise separable convolution, being implemented with different weights for Q , K and V . The depthwise convolution has 256 filters with a spatial dimension of 3×3 . It is applied at a stride of 2 for K and V , and a stride of 1 for Q . This layer is followed in all three cases by a batch normalization layer and a pointwise convolution with 64 filters. The final matrices $Q \in \mathbb{R}^{n_q \times d}$, $K \in \mathbb{R}^{n_k \times d}$ and $V \in \mathbb{R}^{n_v \times d}$ are obtained after flattening the activation maps, while preserving the channel dimension. We note that $n_q = h \cdot w$, $n_k = n_v = \frac{h \cdot w}{4}$ and $d = 64$.

The next stage in the transformer block is the self-attention mechanism, which computes a new value vector for each token as a weighted sum of all value vectors in the set, where the weights are the attention scores. Formally, the operation is defined as follows:

$$Z = \text{softmax} \left(\frac{Q \cdot K^\top}{\sqrt{d_q}} \right) \cdot V, \quad (1)$$

where K^\top is the transpose of K , and Z is a matrix of size $n_q \times d$ containing the new value vectors. We reshape Z into a tensor of $h \times w \times d$ components.

Our network comprises a multi-head attention module, each head containing one convolutional projection and a self-attention mechanism. The tensors resulting from all heads are concatenated along the channel axis, obtaining a tensor Z° of $h \times w \times (d \cdot s)$ components, where s is the number of heads. The tensor Z° is further passed through a pointwise convolutional layer that reduces the number of activation maps to the number of channels c . The tensor P goes through a skip connection, being added to the resulting output, denoted as Z^* .

The final output of the multi-head attention module is fed into a batch normalization layer. To significantly improve efficiency, we replace the multi-layer perceptron that typically follows in a conventional transformer block with two point-

wise convolutional layers. The first pointwise convolutional layer comprises $4 \cdot c$ filters, and the second one only c filters. Another skip connection is added between the input Z^* and the output of this module.

The output of the convolutional transformer is fed into three downscaling heads returning anomaly maps at various resolutions. Each anomaly detection head is formed of two convolutional layers, each with kernels of 3×3 and ReLU activations. The first conv layer is formed of 64 filters. The second conv layer comprises only one filter, and is followed by a pooling layer which returns the output anomaly map at the desired resolution. At inference time, we aggregate the anomaly maps returned by the three heads into a single frame-level anomaly score by computing the maximum value for each map, and averaging the maximum values.

Student pre-training. Our main objective is to transfer the anomaly detection capabilities from teacher networks to our student model. However, if we start the knowledge distillation with random weights for the student, the network must concurrently learn a high-level representation of the training scenes, and replicate the anomaly detection abilities of the teachers. In this scenario, the objective becomes significantly more difficult to complete. Therefore, we propose to independently address the scene understanding task by training the student as an auto-encoder to reconstruct input video frames, before introducing knowledge distillation. More precisely, we train the network to reconstruct the middle frame of a temporal sequence of frames. We fix the length of the temporal sequence to three frames, taken at a stride of t . Given an input sequence $[x^{i-t}, x^i, x^{i+t}]$ and the corresponding output of the auto-encoder $\hat{x}^i = D(E([x^{i-t}, x^i, x^{i+t}]))$, the optimization objective is defined as follows:

$$\mathcal{L}_{\text{AE}} = \frac{1}{h \cdot w \cdot c} \sum_{j=1}^h \sum_{k=1}^w \sum_{l=1}^c (x_{jkl}^i - \hat{x}_{jkl}^i)^2, \quad (2)$$

where E and D represent the encoder and decoder networks. Following Ionescu *et al.* [7], we set $t = 3$ as the temporal step for the input sequence. The encoder E is formed of the initial downsampling block and the convolutional transformer (the multi-scale downsampling blocks are added later, during distillation). The decoder D is composed of transposed convolutions, being symmetric with the downsampling block of the encoder.

Standard knowledge distillation. As the first teacher, denoted as T_1 , we choose the framework based on object-level motion and appearance auto-encoders of Georgescu *et al.* [5]. We select the 3D object-centric network based on self-supervised multi-task learning [4] as the second teacher, denoted as T_2 . The chosen teacher networks [4, 5] predict the anomaly score of each object detected by a pre-trained detector. Hence, an anomaly map containing the anomaly score associated with each bounding box can be obtained for each video frame. Consequently, our first distillation strategy is to

train the student network to regress to the anomaly maps of the teachers, thus learning to imitate the teachers. To make the imitation task more accessible for the student, we lower the resolution of the target anomaly maps by passing them through a max pooling layer. Additionally, we employ multiple resolutions for the anomaly maps, allowing our student model to deal with objects seen at different scales. Let x_T and x_S be the input sequences of frames (centered on some frame x) for the teacher and the student. Let r be the number of output resolutions, and $y = T(x_T)$ and $\hat{y} = S(x_S)$ the anomaly maps of some teacher T and the student S , respectively. For some teacher T , we optimize the following loss function:

$$\mathcal{L}_{\text{KD}}(T, S) = \sum_{k=1}^r \frac{1}{h_k \cdot w_k} \sum_{i=1}^{h_k} \sum_{j=1}^{w_k} (y_{ij}^k - \hat{y}_{ij}^k)^2, \quad (3)$$

where h_k and w_k are the height and the width of the anomaly maps y^k and \hat{y}^k at the k -th resolution. In practice, we set the number of output resolutions to $r = 3$.

Eq. (3) expresses the loss with respect to only one teacher network. However, to increase the generalization power of the student, we distill knowledge from two different anomaly detection models, denoted as T_1 and T_2 . To this end, the objective becomes:

$$\mathcal{L}_{\text{KD}} = \lambda_1 \cdot \mathcal{L}_{\text{KD}}(T_1, S) + \lambda_2 \cdot \mathcal{L}_{\text{KD}}(T_2, S), \quad (4)$$

where λ_1 and λ_2 are the weights for the two losses. In our experiments, we simply set $\lambda_1 = \lambda_2 = 1$ without tuning.

Adversarial distillation. As a second objective for knowledge distillation, we leverage the use of adversarial training, a procedure typically employed to train generative adversarial networks (GANs) [112]. For each teacher involved in the distillation, we introduce a discriminator trained to label the anomaly maps produced by the student as fake examples (class 0) and the ones produced by the teacher as genuine examples (class 1). As mentioned previously, the student outputs multi-resolution anomaly maps. The discriminator receives all anomaly map variants and concatenates them (at the appropriate levels) into a single neural network. Therefore, the discriminator makes a single prediction for all anomaly map resolutions.

Let D_T be the discriminator corresponding to a teacher T . We train D_T and S through a zero-sum game, alternating between minimizing (for S) and maximizing (for D_T) the following loss:

$$\mathcal{L}_{\text{AKD}}(D_T, S) = \mathbb{E}_{x_T \sim p_T} [\log D_T(T(x_T))] + \mathbb{E}_{x_S \sim p_S} [1 - \log D_T(S(x_S))], \quad (5)$$

where x_T and x_S are input sequences of frames for the teacher and the student models, and p_T and p_S are data densities producing samples for the teacher and the student, respectively. We hereby underline that the teacher model T is frozen. Moreover, there is no issue if the data densities p_T and p_S are identical and $x_T = x_S$.

To encapsulate both teachers in the objective formulation, we need to apply Eq. (5) for each discriminator and sum the corresponding losses, as follows:

$$\mathcal{L}_{\text{AKD}} = \mathcal{L}_{\text{AKD}}(D_{T_1}, S) + \mathcal{L}_{\text{AKD}}(D_{T_2}, S), \quad (6)$$

where D_{T_1} and D_{T_2} are the discriminators of teachers T_1 and T_2 , respectively.

Joint distillation. The final objective of our framework combines the losses defined in Eq. (4) and Eq. (6) into a single loss function as follows:

$$\mathcal{L}_{\text{total}} = \mathcal{L}_{\text{KD}} + \alpha \cdot \mathcal{L}_{\text{AKD}}, \quad (7)$$

where the adversarial component receives a fixed weight $\alpha = 0.1$.

4. Experiments

4.1. Data Sets

We conduct experiments on three of the most popular data sets for video anomaly detection: Avenue [40], ShanghaiTech [41] and UCSD Ped2 [42].

Avenue. The Avenue data set [40] includes 16 training videos (15,328 frames) of normal events, and 21 test videos (15,324 frames) with both normal and abnormal situations. The total number of video frames is 30,652.

ShanghaiTech. The ShanghaiTech [41] data set is a much larger data set, containing 330 training videos of normal events, and 107 test videos with normal and abnormal scenes. The total number of frames is about 320K, with over 270K being used for training.

UCSD Ped2. The UCSD Ped2 [42] contains 16 training videos and 12 test videos. As the other two data sets, the training videos depict only normal scenarios.

4.2. Experimental Setup

Teachers. Our frame-level network is trained to replicate the output of two highly effective object-level teachers [4, 5] designed for video anomaly detection. Each teacher uses a pre-trained YOLOv3 [113] to extract objects, which are further processed by an object-centric model. The code to train the teachers is based on the official repositories^{3,4}.

Baselines. We compare our method with state-of-the-art frame-level [6, 8, 11, 13, 15, 17, 18, 20–23, 25, 26, 39, 44, 46, 47, 53, 59–61, 75, 94, 114, 115] and object-level [3–5, 7, 20, 27, 56, 58, 94] frameworks.

Hyperparameters. In all experiments, the student network is configured with $m = 5$ transformer blocks. In each transformer block, the multi-head attention module is based on $s = 5$ heads. The number of output downscaling heads is always 3. For Avenue and ShanghaiTech, the output resolutions are 1×1 , 4×4 and 16×16 . Since the objects in UCSD Ped2 have a much smaller scale, the output resolutions are set to 1×1 , 30×30 and 60×60 . Regardless

³<https://github.com/lilygeorgescu/AED>

⁴<https://github.com/lilygeorgescu/AED-SSMTL>

Table 1. Micro-averaged and macro-averaged frame-level AUC score (in %) of several state-of-the-art frame-level and object-level methods on Avenue, ShanghaiTech and UCSD Ped2. The best scores for each category of methods is highlighted in bold.

Type	Method	Avenue		Shanghai		Ped2	
		AUC					
		Micro	Macro	Micro	Macro	Micro	Macro
Object-centric	Bărbălău <i>et al.</i> [58]	91.6	92.5	83.8	90.5	-	-
	Madan <i>et al.</i> [94] + [58]	91.6	92.4	83.6	90.6	-	-
	Doshi <i>et al.</i> [3]	86.4	-	71.6	-	97.8	-
	Georgescu <i>et al.</i> [4]	91.5	92.8	82.4	90.2	97.5	99.8
	Georgescu <i>et al.</i> [5]	92.3	90.4	82.7	89.3	98.7	99.7
	Ristea <i>et al.</i> [20] + [5]	92.9	91.9	83.6	89.5	-	-
	Madan <i>et al.</i> [94] + [5]	93.2	91.8	83.3	89.3	-	-
	Ionescu <i>et al.</i> [7]	87.4	90.4	78.7	84.9	94.3	97.8
	Wang <i>et al.</i> [56]	92.2	-	84.3	-	99.0	-
Yu <i>et al.</i> [27]	89.6	-	74.8	-	97.3	-	
Frame-level	Astrid <i>et al.</i> [61]	84.7	-	73.7	-	98.4	-
	Astrid <i>et al.</i> [60]	87.1	-	75.9	-	96.5	-
	Gong <i>et al.</i> [6]	83.3	-	71.2	-	94.1	-
	Ionescu <i>et al.</i> [8]	88.9	-	-	-	-	-
	Lee <i>et al.</i> [11]	90.0	-	-	-	96.6	-
	Liu <i>et al.</i> [75]	84.4	-	-	-	87.5	-
	Liu <i>et al.</i> [39]	85.1	81.7	72.8	80.6	95.4	-
	Liu <i>et al.</i> [13]	89.9	93.5	74.2	83.2	99.3	-
	Madan <i>et al.</i> [94] + [13]	89.5	93.6	75.2	83.8	-	-
	Madan <i>et al.</i> [94] + [39]	89.1	84.8	74.6	83.3	-	-
	Madan <i>et al.</i> [94] + [17]	86.4	86.3	70.6	80.3	-	-
	Nguyen <i>et al.</i> [15]	86.9	-	-	-	96.2	-
	Park <i>et al.</i> [17]	82.8	86.8	68.3	79.7	97.0	-
	Park <i>et al.</i> [57]	85.3	-	72.2	-	96.3	-
	Ramachandra <i>et al.</i> [18]	72.0	-	-	-	88.3	-
	Ramachandra <i>et al.</i> [44]	87.2	-	-	-	93.0	-
	Ravanbakhsh <i>et al.</i> [47]	-	-	-	-	93.5	-
	Ravanbakhsh <i>et al.</i> [46]	-	-	-	-	88.4	-
	Ristea <i>et al.</i> [20] + [39]	87.3	84.5	74.5	82.9	-	-
	Ristea <i>et al.</i> [20] + [13]	90.9	92.2	75.5	83.7	-	-
	Ristea <i>et al.</i> [20] + [17]	84.8	88.6	69.8	80.2	-	-
	Smeureanu <i>et al.</i> [21]	84.6	-	-	-	-	-
	Sultani <i>et al.</i> [114]	-	-	-	76.5	-	-
	Sun <i>et al.</i> [22]	89.6	-	74.7	-	-	-
	Tang <i>et al.</i> [23]	85.1	-	73.0	-	96.3	-
	Wang <i>et al.</i> [25]	87.0	-	79.3	-	-	-
	Wu <i>et al.</i> [115]	-	-	80.4	-	-	-
	Wu <i>et al.</i> [26]	86.6	-	-	-	96.9	-
	Yu <i>et al.</i> [59]	90.2	-	-	-	97.3	-
	Zhang <i>et al.</i> [53]	-	-	-	-	91.0	-
	Ours	88.2	87.7	77.9	86.0	93.6	97.0

of the dataset, the student network is trained for 35 epochs with mini-batches of 64 video sequences of three frames each. We optimize the model with Adam [116], using a learning rate of 10^{-4} and a weight decay set to 10^{-5} (all other hyperparameters are set to the default values).

Evaluation. Following recent works [1, 5, 20], we evaluate

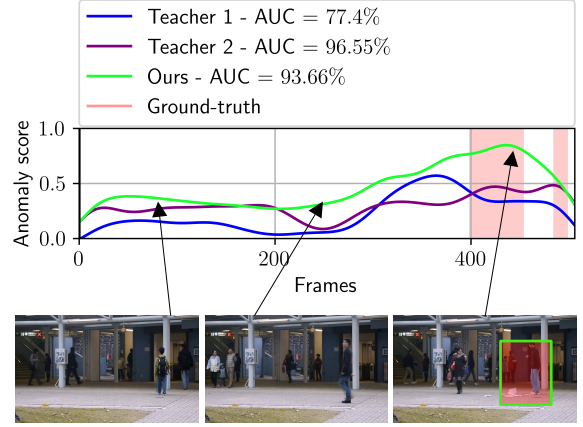


Figure 4. Comparing the frame-level anomaly scores of teachers T_1 [5] and T_2 [4] with the scores of our student on test video 14 from Avenue. The anomaly localization examples are provided by the head with the highest resolution of our student. Best viewed in color.

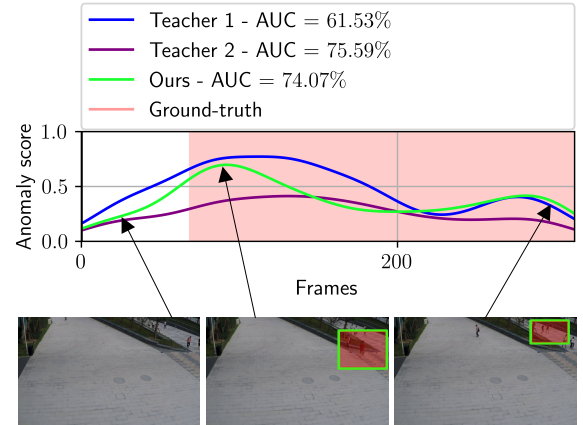


Figure 5. Comparing the frame-level anomaly scores of teachers T_1 [5] and T_2 [4] with the scores of our student on test video 01_0055 from ShanghaiTech. The anomaly localization examples are provided by the head with the highest resolution of our student. Best viewed in color.

models in terms of the micro-averaged and macro-averaged frame-level AUC. For both measures, we compute the area under the ROC curve (AUC) with respect to the ground-truth frame-level annotations. A frame is labeled as abnormal if the predicted anomaly score is larger than a given threshold. For the micro AUC, all the test frames are first concatenated into a single video before computing the AUC. For the macro AUC, we compute the AUC of each test video and report the mean of the resulting AUC scores.

4.3. Results

In Table 1, we present the micro and macro AUC scores of our method in comparison with the state-of-the-art frame-level and object-level methods on the Avenue, ShanghaiTech and UCSD Ped2 benchmarks.

Avenue. Even if our method is below the top scoring object-

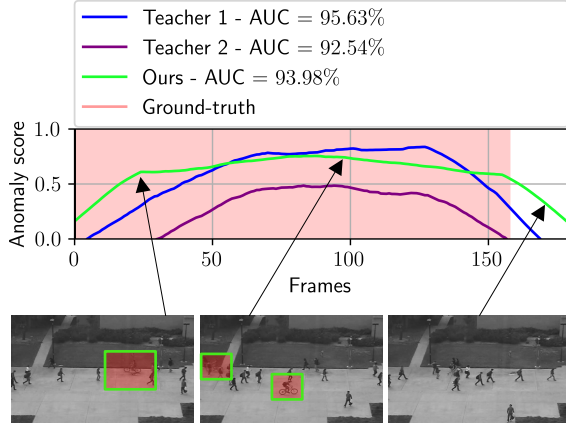


Figure 6. Comparing the frame-level anomaly scores of teachers T_1 [5] and T_2 [4] with the scores of our student on test video 6 from UCSD Ped2. The anomaly localization examples are produced by the head with the highest resolution of our student. Best viewed in color.

centric methods, it yields comparable performance with some object-level methods, *e.g.* [7, 27]. Moreover, with a micro AUC of 88.2%, our student outperforms most of the frame-based models. In Figure 4, we illustrate the anomaly detection performance on test video 14 from Avenue. Our student is able to surpass the lower results of teacher T_1 , being very close to teacher T_2 . This shows the importance of learning from more than one teacher.

ShanghaiTech. Among all frame-level frameworks reporting results on ShanghaiTech, we observe that our model ranks first in terms of the macro AUC, and third in terms of the micro AUC. With respect to the teachers [4, 5], our micro and macro AUC drops are lower than 5%. In Figure 5, we showcase the anomaly detection performance on test video 01_0055 from ShanghaiTech. Our student, being trained to mimic both teachers, is able to surpass the lower results of teacher T_1 , getting close to the performance of teacher T_2 .

UCSD Ped2. In terms of the macro AUC on UCSD Ped2, our model is just below the state-of-the-art object-centric approach [5], at a difference of only 2.8%. In terms of the micro AUC, the student registers a performance drop of at most 5.1% with respect to both teachers [4, 5]. In Figure 6, we present the anomaly detection performance on test video 6 from UCSD Ped2. Once again, the performance of our student is between that of the teachers T_1 and T_2 .

Speed versus accuracy trade-off. In Figures 2 and 7, we compare our model with several recent frame-level and object-centric methods in terms of the trade-off between accuracy and speed, on ShanghaiTech and Avenue, respectively. The running times of all methods [4–6, 9, 13, 17, 20, 39, 56, 57], including our own, are measured on a machine with an Nvidia GeForce GTX 3090 GPU with 24 GB of VRAM. The FPS rates of the object-level methods range between 20 and 52. Some frame-level methods are comparatively faster,

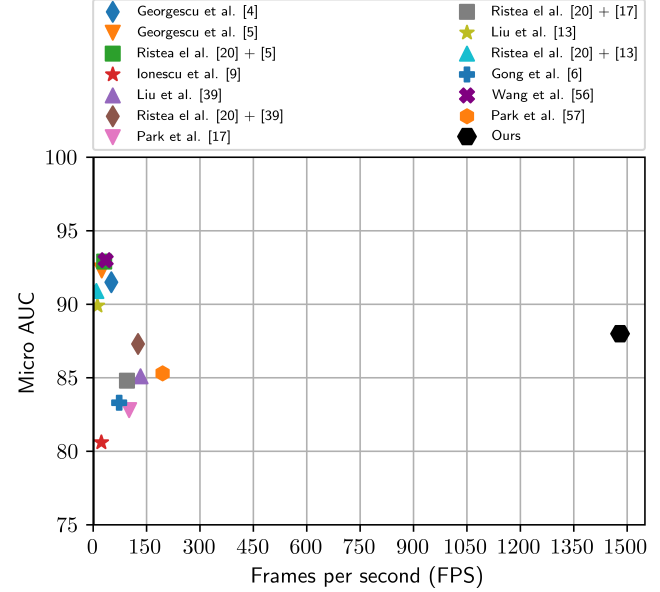


Figure 7. The trade-off between performance (micro AUC) and speed (FPS) for our student versus multiple state-of-the-art methods [4–6, 9, 13, 17, 20, 39, 56, 57] (with available code), on the Avenue data set. The running times of all methods are measured on a machine with an Nvidia GeForce GTX 3090 GPU with 24 GB of VRAM. Best viewed in color.

the most efficient one, proposed by Park *et al.* [57], running at 195 FPS. Our method runs at 1480 FPS, being more than 7 times faster than the most efficient competitor [57]. Our significant speed gains come at small performance cost, falling only 5% behind the state-of-the-art teachers [4, 5].

Ablation study. We present a comprehensive set of ablation results in the supplementary.

5. Conclusion

In this paper, we introduced a novel teacher-student framework for anomaly detection in video, learning to detect anomalies by distilling knowledge from multiple highly accurate object-level teachers into a highly efficient student. Moreover, we proposed adversarial knowledge distillation in the context of anomaly detection, introducing an adversarial discriminator for each teacher. With our framework, we successfully trained an efficient convolutional transformer, obtaining a state-of-the-art speed versus performance trade-off. More precisely, we obtained an unprecedented speed of 1480 FPS, with a minimal performance decrease. In future work, we aim to further raise the accuracy of our student by introducing more teachers and tasks.

Acknowledgments

This work was supported by a grant of the Romanian Ministry of Education and Research, CNCS - UEFISCDI, project number PN-III-P2-2.1-PED-2021-0195, within PNCDI III.

References

- [1] Andra Acsintoae, Andrei Florescu, Mariana-Iuliana Georgescu, Tudor Mare, Paul Sumedrea, Radu Tudor Ionescu, Fahad Shahbaz Khan, and Mubarak Shah, “Ubnormal: New benchmark for supervised open-set video anomaly detection,” in *Proceedings of CVPR*, 2022, pp. 20143–20153. 1, 7
- [2] Fei Dong, Yu Zhang, and Xiushan Nie, “Dual Discriminator Generative Adversarial Network for Video Anomaly Detection,” *IEEE Access*, vol. 8, pp. 88170–88176, 2020. 1, 2
- [3] Keval Doshi and Yasin Yilmaz, “Any-Shot Sequential Anomaly Detection in Surveillance Videos,” in *Proceedings of CVPRW*, 2020, pp. 934–935. 1, 2, 6, 7
- [4] Mariana-Iuliana Georgescu, Antonio Bărbălău, Radu Tudor Ionescu, Fahad Shahbaz Khan, Marius Popescu, and Mubarak Shah, “Anomaly Detection in Video via Self-Supervised and Multi-Task Learning,” in *Proceedings of CVPR*, 2021, pp. 12742–12752. 1, 2, 3, 4, 5, 6, 7, 8, 15, 16, 17, 18
- [5] Mariana Iuliana Georgescu, Radu Ionescu, Fahad Shahbaz Khan, Marius Popescu, and Mubarak Shah, “A Background-Agnostic Framework with Adversarial Training for Abnormal Event Detection in Video,” *IEEE Transactions on Pattern Analysis and Machine Intelligence*, vol. 44, no. 9, pp. 4505–4523, 2022. 1, 2, 3, 4, 5, 6, 7, 8, 15, 16, 17, 18
- [6] Dong Gong, Lingqiao Liu, Vuong Le, Budhaditya Saha, Moussa Reda Mansour, Svetha Venkatesh, and Anton Van Den Hengel, “Memorizing Normality to Detect Anomaly: Memory-Augmented Deep Autoencoder for Unsupervised Anomaly Detection,” in *Proceedings of ICCV*, 2019, pp. 1705–1714. 1, 2, 3, 6, 7, 8
- [7] Radu Tudor Ionescu, Fahad Shahbaz Khan, Mariana-Iuliana Georgescu, and Ling Shao, “Object-Centric Auto-Encoders and Dummy Anomalies for Abnormal Event Detection in Video,” in *Proceedings of CVPR*, 2019, pp. 7842–7851. 1, 2, 3, 5, 6, 7, 8
- [8] Radu Tudor Ionescu, Sorina Smeureanu, Marius Popescu, and Bogdan Alexe, “Detecting abnormal events in video using Narrowed Normality Clusters,” in *Proceedings of WACV*, 2019, pp. 1951–1960. 1, 2, 6, 7
- [9] Radu Tudor Ionescu, Sorina Smeureanu, Bogdan Alexe, and Marius Popescu, “Unmasking the abnormal events in video,” in *Proceedings of ICCV*, 2017, pp. 2895–2903. 1, 2, 8
- [10] Xiangli Ji, Bairong Li, and Yuesheng Zhu, “TAM-Net: Temporal Enhanced Appearance-to-Motion Generative Network for Video Anomaly Detection,” in *Proceedings of IJCNN*, 2020, pp. 1–8. 1
- [11] Sangmin Lee, Hak Gu Kim, and Yong Man Ro, “BMAN: Bidirectional Multi-Scale Aggregation Networks for Abnormal Event Detection,” *IEEE Transactions on Image Processing*, vol. 29, pp. 2395–2408, 2019. 1, 2, 4, 6, 7
- [12] Guoqiu Li, Guanxiong Cai, Xingyu Zeng, and Rui Zhao, “Scale-Aware Spatio-Temporal Relation Learning for Video Anomaly Detection,” in *Proceedings of ECCV*, 2022, pp. 333–350. 1
- [13] Zhian Liu, Yongwei Nie, Chengjiang Long, Qing Zhang, and Guiqing Li, “A Hybrid Video Anomaly Detection Framework via Memory-Augmented Flow Reconstruction and Flow-Guided Frame Prediction,” in *Proceedings of ICCV*, 2021, pp. 13588–13597. 1, 2, 3, 6, 7, 8
- [14] Yiwei Lu, Frank Yu, Mahesh Kumar, Krishna Reddy, and Yang Wang, “Few-Shot Scene-Adaptive Anomaly Detection,” in *Proceedings of ECCV*, 2020, pp. 125–141. 1
- [15] Trong-Nguyen Nguyen and Jean Meunier, “Anomaly Detection in Video Sequence With Appearance-Motion Correspondence,” in *Proceedings of ICCV*, 2019, pp. 1273–1283. 1, 2, 6, 7
- [16] Guansong Pang, Cheng Yan, Chunhua Shen, Anton van den Hengel, and Xiao Bai, “Self-trained Deep Ordinal Regression for End-to-End Video Anomaly Detection,” in *Proceedings of CVPR*, 2020, pp. 12173–12182. 1, 2
- [17] Hyunjong Park, Jongyoun Noh, and Bumsub Ham, “Learning Memory-guided Normality for Anomaly Detection,” in *Proceedings of CVPR*, 2020, pp. 14372–14381. 1, 2, 3, 6, 7, 8
- [18] Bharathkumar Ramachandra and Michael Jones, “Street Scene: A new dataset and evaluation protocol for video anomaly detection,” in *Proceedings of WACV*, 2020, pp. 2569–2578. 1, 2, 6, 7
- [19] Bharathkumar Ramachandra, Michael J. Jones, and Ranga Raju Vatsavai, “A Survey of Single-Scene Video Anomaly Detection,” *IEEE Transactions on Pattern Analysis and Machine Intelligence*, 2020. 1, 2
- [20] Nicolae-Cătălin Ristea, Neelu Madan, Radu Tudor Ionescu, Kamal Nasrollahi, Fahad Shahbaz Khan,

- Thomas B. Moeslund, and Mubarak Shah, “Self-Supervised Predictive Convolutional Attentive Block for Anomaly Detection,” in *Proceedings of CVPR*, 2022, pp. 13576–13586. 1, 2, 3, 6, 7, 8
- [21] Sorina Smeureanu, Radu Tudor Ionescu, Marius Popescu, and Bogdan Alexe, “Deep Appearance Features for Abnormal Behavior Detection in Video,” in *Proceedings of ICIAP*, 2017, vol. 10485, pp. 779–789. 1, 2, 6, 7
- [22] Che Sun, Yunde Jia, Yao Hu, and Yuwei Wu, “Scene-Aware Context Reasoning for Unsupervised Abnormal Event Detection in Videos,” in *Proceedings of ACMMM*, 2020, pp. 184–192. 1, 2, 6, 7
- [23] Yao Tang, Lin Zhao, Shanshan Zhang, Chen Gong, Guangyu Li, and Jian Yang, “Integrating prediction and reconstruction for anomaly detection,” *Pattern Recognition Letters*, vol. 129, pp. 123–130, 2020. 1, 2, 6, 7
- [24] Hung Vu, Tu Dinh Nguyen, Trung Le, Wei Luo, and Dinh Phung, “Robust Anomaly Detection in Videos Using Multilevel Representations,” in *Proceedings of AAAI*, 2019, vol. 33, pp. 5216–5223. 1
- [25] Ziming Wang, Yuexian Zou, and Zeming Zhang, “Cluster Attention Contrast for Video Anomaly Detection,” in *Proceedings of ACMMM*, 2020, pp. 2463–2471. 1, 6, 7
- [26] Peng Wu, Jing Liu, and Fang Shen, “A Deep One-Class Neural Network for Anomalous Event Detection in Complex Scenes,” *IEEE Transactions on Neural Networks and Learning Systems*, vol. 31, no. 7, pp. 2609–2622, 2019. 1, 2, 6, 7
- [27] Guang Yu, Siqi Wang, Zhiping Cai, En Zhu, Chuanfu Xu, Jianping Yin, and Marius Kloft, “Cloze Test Helps: Effective Video Anomaly Detection via Learning to Complete Video Events,” in *Proceedings of ACMMM*, 2020, pp. 583–591. 1, 2, 3, 6, 7, 8
- [28] Xumin Yu, Lulu Tang, Yongming Rao, Tiejun Huang, Jie Zhou, and Jiwen Lu, “Point-BERT: Pre-Training 3D Point Cloud Transformers With Masked Point Modeling,” in *Proceedings of CVPR*, 2022, pp. 19313–19322. 1
- [29] Muhammad Zaigham Zaheer, Jin-ha Lee, Marcella Astrid, and Seung-Ik Lee, “Old is Gold: Redefining the Adversarially Learned One-Class Classifier Training Paradigm,” in *Proceedings of CVPR*, 2020, pp. 14183–14193. 1
- [30] Muhammad Zaigham Zaheer, Arif Mahmood, Marcella Astrid, and Seung-Ik Lee, “CLAWS: Clustering Assisted Weakly Supervised Learning with Normalcy Suppression for Anomalous Event Detection,” in *Proceedings of ECCV*, 2020, pp. 358–376. 1
- [31] Muhammad Zaigham Zaheer, Arif Mahmood, Haris M. Khan, Mattia Segu, Fisher Yu, and Seung-Ik Lee, “Generative Cooperative Learning for Unsupervised Video Anomaly Detection,” in *Proceedings of CVPR*, 2022, pp. 14744–14754. 1
- [32] Borislav Antic and Bjorn Ommer, “Video parsing for abnormality detection,” in *Proceedings of ICCV*, 2011, pp. 2415–2422. 2
- [33] Kai-Wen Cheng, Yie-Tarng Chen, and Wen-Hsien Fang, “Video anomaly detection and localization using hierarchical feature representation and Gaussian process regression,” in *Proceedings of CVPR*, 2015, pp. 2909–2917. 2
- [34] Y. Cong, J. Yuan, and J. Liu, “Sparse reconstruction cost for abnormal event detection,” in *Proceedings of CVPR*, 2011, pp. 3449–3456. 2
- [35] Jayanta K. Dutta and Bonny Banerjee, “Online Detection of Abnormal Events Using Incremental Coding Length,” in *Proceedings of AAAI*, 2015, pp. 3755–3761. 2
- [36] Mahmudul Hasan, Jonghyun Choi, Jan Neumann, Amit K. Roy-Chowdhury, and Larry S. Davis, “Learning temporal regularity in video sequences,” in *Proceedings of CVPR*, 2016, pp. 733–742. 2
- [37] Jaechul Kim and Kristen Grauman, “Observe locally, infer globally: A space-time MRF for detecting abnormal activities with incremental updates,” in *Proceedings of CVPR*, 2009, pp. 2921–2928. 2
- [38] Weixin Li, Vijay Mahadevan, and Nuno Vasconcelos, “Anomaly detection and localization in crowded scenes,” *IEEE Transactions on Pattern Analysis and Machine Intelligence*, vol. 36, no. 1, pp. 18–32, 2014. 2
- [39] Wen Liu, Weixin Luo, Dongze Lian, and Shenghua Gao, “Future Frame Prediction for Anomaly Detection – A New Baseline,” in *Proceedings of CVPR*, 2018, pp. 6536–6545. 2, 3, 4, 6, 7, 8
- [40] Cewu Lu, Jianping Shi, and Jiaya Jia, “Abnormal Event Detection at 150 FPS in MATLAB,” in *Proceedings of ICCV*, 2013, pp. 2720–2727. 2, 6, 15, 16, 17

- [41] Weixin Luo, Wen Liu, and Shenghua Gao, “A Revisit of Sparse Coding Based Anomaly Detection in Stacked RNN Framework,” in *Proceedings of ICCV*, 2017, pp. 341–349. 2, 6, 17
- [42] Vijay Mahadevan, Wei-Xin LI, Viral Bhalodia, and Nuno Vasconcelos, “Anomaly Detection in Crowded Scenes,” in *Proceedings of CVPR*, 2010, pp. 1975–1981. 2, 6, 17
- [43] Ramin Mehran, Alexis Oyama, and Mubarak Shah, “Abnormal crowd behavior detection using social force model,” in *Proceedings of CVPR*, 2009, pp. 935–942. 2
- [44] Bharathkumar Ramachandra, Michael Jones, and Ranga Vatsavai, “Learning a distance function with a Siamese network to localize anomalies in videos,” in *Proceedings of WACV*, 2020, pp. 2598–2607. 2, 6, 7
- [45] Bharathkumar Ramachandra, Michael Jones, and Ranga Raju Vatsavai, “Perceptual metric learning for video anomaly detection,” *Machine Vision and Applications*, vol. 32, pp. 1432–1769, 2021. 2
- [46] Mahdyar Ravanbakhsh, Moin Nabi, Hossein Mousavi, Enver Sangineto, and Nicu Sebe, “Plug-and-Play CNN for Crowd Motion Analysis: An Application in Abnormal Event Detection,” in *Proceedings of WACV*, 2018, pp. 1689–1698. 2, 6, 7
- [47] Mahdyar Ravanbakhsh, Moin Nabi, Enver Sangineto, Lucio Marcenaro, Carlo Regazzoni, and Nicu Sebe, “Abnormal Event Detection in Videos using Generative Adversarial Nets,” in *Proceedings of ICIP*, 2017, pp. 1577–1581. 2, 6, 7
- [48] Huamin Ren, Weifeng Liu, Soren Ingvor Olsen, Sergio Escalera, and Thomas B. Moeslund, “Unsupervised Behavior-Specific Dictionary Learning for Abnormal Event Detection,” in *Proceedings of BMVC*, 2015, pp. 28.1–28.13. 2
- [49] Mohammad Sabokrou, Mohsen Fayyaz, Mahmood Fathy, and Reinhard Klette, “Deep-Cascade: Cascading 3D Deep Neural Networks for Fast Anomaly Detection and Localization in Crowded Scenes,” *IEEE Transactions on Image Processing*, vol. 26, no. 4, pp. 1992–2004, 2017. 2
- [50] Dan Xu, Yan Yan, Elisa Ricci, and Nicu Sebe, “Detecting Anomalous Events in Videos by Learning Deep Representations of Appearance and Motion,” *Computer Vision and Image Understanding*, vol. 156, pp. 117–127, 2017. 2
- [51] Bin Zhao, Li Fei-Fei, and Eric P. Xing, “Online Detection of Unusual Events in Videos via Dynamic Sparse Coding,” in *Proceedings of CVPR*, 2011, pp. 3313–3320. 2
- [52] Xinfeng Zhang, Su Yang, Jiulong Zhang, and Weishan Zhang, “Video Anomaly Detection and Localization using Motion-field Shape Description and Homogeneity Testing,” *Pattern Recognition*, p. 107394, 2020. 2
- [53] Ying Zhang, Huchuan Lu, Lihe Zhang, Xiang Ruan, and Shun Sakai, “Video anomaly detection based on locality sensitive hashing filters,” *Pattern Recognition*, vol. 59, pp. 302–311, 2016. 2, 6, 7
- [54] Jia-Xing Zhong, Nannan Li, Weijie Kong, Shan Liu, Thomas H. Li, and Ge Li, “Graph Convolutional Label Noise Cleaner: Train a Plug-And-Play Action Classifier for Anomaly Detection,” in *Proceedings of CVPR*, 2019, pp. 1237–1246. 2
- [55] Yaxiang Fan, Gongjian Wen, Deren Li, Shaohua Qiu, Martin D. Levine, and Fei Xiao, “Video anomaly detection and localization via Gaussian Mixture Fully Convolutional Variational Autoencoder,” *Computer Vision and Image Understanding*, vol. 195, pp. 102920, 2020. 2
- [56] Guodong Wang, Yunhong Wang, Jie Qin, Dongming Zhang, Xiuguo Bao, and Di Huang, “Video anomaly detection by solving decoupled spatio-temporal jigsaw puzzles,” in *Proceedings of ECCV*, 2022, pp. 494–511. 2, 3, 6, 7, 8
- [57] Chaewon Park, MyeongAh Cho, Minhyeok Lee, and Sangyoun Lee, “FastAno: Fast anomaly detection via spatio-temporal patch transformation,” in *Proceedings of WACV*, 2022, pp. 2249–2259. 2, 3, 7, 8
- [58] Antonio Bărbălău, Radu Tudor Ionescu, Mariana-Iuliana Georgescu, Jacob Dueholm, Bharathkumar Ramachandra, Kamal Nasrollahi, Fahad Shahbaz Khan, Thomas B Moeslund, and Mubarak Shah, “SSMTL++: Revisiting Self-Supervised Multi-Task Learning for Video Anomaly Detection,” *arXiv preprint arXiv:2207.08003*, 2022. 2, 3, 6, 7
- [59] Jongmin Yu, Younkwan Lee, Kin Choong Yow, Moongu Jeon, and Witold Pedrycz, “Abnormal event detection and localization via adversarial event prediction,” *IEEE Transactions on Neural Networks and Learning Systems*, vol. 33, no. 8, pp. 3572–3586, 2022. 2, 3, 6, 7

- [60] Marcella Astrid, Muhammad Zaigham Zaheer, Jae-Yeong Lee, and Seung-Ik Lee, "Learning not to reconstruct anomalies," in *Proceedings of BMVC*, 2021. 2, 6, 7
- [61] Marcella Astrid, Muhammad Zaigham Zaheer, and Seung-Ik Lee, "Synthetic Temporal Anomaly Guided End-to-End Video Anomaly Detection," in *Proceedings of ICCVW*, 2021, pp. 207–214. 2, 6, 7
- [62] Guansong Pang, Chunhua Shen, Longbing Cao, and Anton Van Den Hengel, "Deep learning for anomaly detection: A review," *ACM Computing Surveys*, vol. 54, no. 2, pp. 1–38, 2021. 2
- [63] Amit Adam, Ehud Rivlin, Ilan Shimshoni, and Daviv Reinitz, "Robust Real-Time Unusual Event Detection Using Multiple Fixed-Location Monitors," *IEEE Transactions on Pattern Analysis and Machine Intelligence*, vol. 30, no. 3, pp. 555–560, 2008. 2
- [64] Yachuang Feng, Yuan Yuan, and Xiaoqiang Lu, "Learning deep event models for crowd anomaly detection," *Neurocomputing*, vol. 219, pp. 548–556, 2017. 2
- [65] Ryota Hinami, Tao Mei, and Shin'ichi Satoh, "Joint Detection and Recounting of Abnormal Events by Learning Deep Generic Knowledge," in *Proceedings of ICCV*, 2017, pp. 3639–3647. 2
- [66] Babak Saleh, Ali Farhadi, and Ahmed Elgammal, "Object-Centric Anomaly Detection by Attribute-Based Reasoning," in *Proceedings of CVPR*, 2013, pp. 787–794. 2
- [67] Shandong Wu, Brian E. Moore, and Mubarak Shah, "Chaotic Invariants of Lagrangian Particle Trajectories for Anomaly Detection in Crowded Scenes," in *Proceedings of CVPR*, 2010, pp. 2054–2060. 2
- [68] Mohammad Sabokrou, Mohsen Fayyaz, Mahmood Fathy, Zahra Moayed, and Reinhard Klette, "Deep-Anomaly: Fully Convolutional Neural Network for Fast Anomaly Detection in Crowded Scenes," *Computer Vision and Image Understanding*, vol. 172, pp. 88–97, 2018. 2
- [69] Venkatesh Saligrama and Zhu Chen, "Video anomaly detection based on local statistical aggregates," in *Proceedings of CVPR*, 2012, pp. 2112–2119. 2
- [70] Qianru Sun, Hong Liu, and Tatsuya Harada, "Online growing neural gas for anomaly detection in changing surveillance scenes," *Pattern Recognition*, vol. 64, no. C, pp. 187–201, Apr. 2017. 2
- [71] Hanh T.M. Tran and David Hogg, "Anomaly Detection using a Convolutional Winner-Take-All Autoencoder," in *Proceedings of BMVC*, 2017. 2
- [72] Ye Fei, Chaoqin Huang, Cao Jinkun, Maosen Li, Ya Zhang, and Cewu Lu, "Attribute Restoration Framework for Anomaly Detection," *IEEE Transactions on Multimedia*, vol. 24, pp. 116–127, 2022. 2
- [73] Zhenyu Li, Ning Li, Kaitao Jiang, Zhiheng Ma, Xing Wei, Xiaopeng Hong, and Yihong Gong, "Superpixel Masking and Inpainting for Self-Supervised Anomaly Detection," in *Proceedings of BMVC*, 2020. 2
- [74] Allison Del Giorno, J. Andrew Bagnell, and Martial Hebert, "A Discriminative Framework for Anomaly Detection in Large Videos," in *Proceedings of ECCV*, 2016, pp. 334–349. 2
- [75] Yusha Liu, Chun-Liang Li, and Barnabás Póczos, "Classifier Two-Sample Test for Video Anomaly Detections," in *Proceedings of BMVC*, 2018. 2, 6, 7
- [76] Keval Doshi and Yasin Yilmaz, "Continual Learning for Anomaly Detection in Surveillance Videos," in *Proceedings of CVPRW*, 2020, pp. 254–255. 2
- [77] Bo Li, Sam Leroux, and Pieter Simoons, "Decoupled appearance and motion learning for efficient anomaly detection in surveillance video," *Computer Vision and Image Understanding*, vol. 210, pp. 103249, 2021. 3
- [78] Zhiwen Fang, Joey Tianyi Zhou, Yang Xiao, Yanan Li, and Feng Yang, "Multi-encoder towards effective anomaly detection in videos," *IEEE Transactions on Multimedia*, vol. 23, pp. 4106–4116, 2020. 3
- [79] Keval Doshi and Yasin Yilmaz, "An efficient approach for anomaly detection in traffic videos," in *Proceedings of CVPR*, 2021, pp. 4236–4244. 3
- [80] Ashish Vaswani, Noam Shazeer, Niki Parmar, Jakob Uszkoreit, Llion Jones, Aidan N. Gomez, Łukasz Kaiser, and Illia Polosukhin, "Attention is all you need," in *Proceedings of NIPS*, 2017, vol. 30, pp. 6000–6010. 3
- [81] Nicolas Carion, Francisco Massa, Gabriel Synnaeve, Nicolas Usunier, Alexander Kirillov, and Sergey Zagoruyko, "End-to-end object detection with transformers," in *Proceedings of ECCV*, 2020, pp. 213–229. 3
- [82] Jieneng Chen, Yongyi Lu, Qihang Yu, Xiangde Luo, Ehsan Adeli, Yan Wang, Le Lu, Alan L. Yuille, and Yuyin Zhou, "TransUNet: Transformers Make Strong

Encoders for Medical Image Segmentation,” *arXiv preprint arXiv:2102.04306*, 2021. 3

- [83] Alexey Dosovitskiy, Lucas Beyer, Alexander Kolesnikov, Dirk Weissenborn, Xiaohua Zhai, Thomas Unterthiner, Mostafa Dehghani, Matthias Minderer, Georg Heigold, Sylvain Gelly, Jakob Uszkoreit, and Neil Houlsby, “An image is worth 16x16 words: Transformers for image recognition at scale,” in *Proceedings of ICLR*, 2021. 3
- [84] Salman Khan, Muzammal Naseer, Munawar Hayat, Syed Waqas Zamir, Fahad Shahbaz Khan, and Mubarak Shah, “Transformers in Vision: A Survey,” *ACM Computing Surveys*, vol. 54, no. 10s, 2022. 3
- [85] Niki Parmar, Ashish Vaswani, Jakob Uszkoreit, Lukasz Kaiser, Noam Shazeer, Alexander Ku, and Dustin Tran, “Image transformer,” in *Proceedings of ICML*, 2018, pp. 4055–4064. 3
- [86] Nicolae-Catalin Ristea, Andreea-Iuliana Miron, Olivian Savencu, Mariana-Iuliana Georgescu, Nicolae Verga, Fahad Shahbaz Khan, and Radu Tudor Ionescu, “CyTran: Cycle-Consistent Transformers for Non-Contrast to Contrast CT Translation,” *arXiv preprint arXiv:2110.06400*, 2021. 3
- [87] Hugo Touvron, Matthieu Cord, Matthijs Douze, Francisco Massa, Alexandre Sablayrolles, and Hervé Jégou, “Training data-efficient image transformers & distillation through attention,” in *Proceedings of ICML*, 2021, pp. 10347–10357. 3
- [88] Haiping Wu, Bin Xiao, Noel Codella, Mengchen Liu, Xiyang Dai, Lu Yuan, and Lei Zhang, “CvT: Introducing Convolutions to Vision Transformers,” in *Proceedings of ICCV*, 2021, pp. 22–31. 3, 4, 5, 17
- [89] Xiaogang Xu and Ning Xu, “Hierarchical Image Generation via Transformer-Based Sequential Patch Selection,” in *Proceedings of AAAI*, 2022, pp. 2938–2945. 3
- [90] Bowen Zhang, Shuyang Gu, Bo Zhang, Jianmin Bao, Dong Chen, Fang Wen, Yong Wang, and Baining Guo, “StyleSwin: Transformer-based GAN for High-resolution Image Generation,” in *Proceedings of CVPR*, 2022, pp. 11304–11314. 3
- [91] Minghang Zheng, Peng Gao, Xiaogang Wang, Hongsheng Li, and Hao Dong, “End-to-end object detection with adaptive clustering transformer,” in *Proceedings of BMVC*, 2020. 3
- [92] Xizhou Zhu, Weijie Su, Lewei Lu, Bin Li, Xiaogang Wang, and Jifeng Dai, “Deformable DETR: Deformable Transformers for End-to-End Object Detection,” in *Proceedings of ICLR*, 2020. 3
- [93] Pu Jin, Lichao Mou, Gui-Song Xia, and Xiao Xiang Zhu, “Anomaly detection in aerial videos with transformers,” *IEEE Transactions on Geoscience and Remote Sensing*, vol. 60, pp. 1–13, 2022. 3
- [94] Neelu Madan, Nicolae-Catalin Ristea, Radu Tudor Ionescu, Kamal Nasrollahi, Fahad Shahbaz Khan, Thomas B Moeslund, and Mubarak Shah, “Self-supervised masked convolutional transformer block for anomaly detection,” *arXiv preprint arXiv:2209.12148*, 2022. 3, 6, 7
- [95] Liyang Chen, Zhiyuan You, Nian Zhang, Juntong Xi, and Xinyi Le, “UTRAD: Anomaly detection and localization with U-Transformer,” *Neural Networks*, vol. 147, pp. 53–62, 2022. 3
- [96] Hongchun Yuan, Zhenyu Cai, Hui Zhou, Yue Wang, and Xiangzhi Chen, “TransAnomaly: Video Anomaly Detection Using Video Vision Transformer,” *IEEE Access*, vol. 9, pp. 123977–123986, 2021. 3
- [97] Jimmy Ba and Rich Caruana, “Do deep nets really need to be deep?,” in *Proceedings of NIPS*, 2014, pp. 2654–2662. 3
- [98] Geoffrey Hinton, Oriol Vinyals, and Jeffrey Dean, “Distilling the Knowledge in a Neural Network,” in *Proceedings of NIPS Deep Learning and Representation Learning Workshop*, 2014. 3
- [99] Jianping Gou, Baosheng Yu, Stephen J. Maybank, and Dacheng Tao, “Knowledge distillation: A survey,” *International Journal of Computer Vision*, vol. 129, no. 6, pp. 1789–1819, 2021. 3
- [100] Inseop Chung, Seonguk Park, Jangho Kim, and Nojun Kwak, “Feature-map-level online adversarial knowledge distillation,” in *Proceedings of ICML*, 2020, vol. 119, pp. 2006–2015. 4
- [101] Wonpyo Park, Dongju Kim, Yan Lu, and Minsu Cho, “Relational Knowledge Distillation,” in *Proceedings of CVPR*, 2019, pp. 3962–3971. 4
- [102] Junho Yim, Donggyu Joo, Jihoon Bae, and Junmo Kim, “A Gift from Knowledge Distillation: Fast Optimization, Network Minimization and Transfer Learning,” in *Proceedings of CVPR*, 2017, pp. 7130–7138. 4
- [103] Lu Yu, Vacit Oguz Yazici, Xialei Liu, Joost van de Weijer, Yongmei Cheng, and Arnau Ramisa, “Learning Metrics from Teachers: Compact Networks for

- Image Embedding,” in *Proceedings of CVPR*, 2019, pp. 2907–2916. 4
- [104] Yushu Feng, Huan Wang, Roland Hu, and Daniel T Yi, “Triplet distillation for deep face recognition,” in *Proceedings of ICIP*, 2020, pp. 808–812. 4
- [105] Mariana-Iuliana Georgescu, Georgian-Emilian Duțun-defined, and Radu Tudor Ionescu, “Teacher–student training and triplet loss to reduce the effect of drastic face occlusion: Application to emotion recognition, gender identification and age estimation,” *Machine Vision and Applications*, vol. 33, no. 1, pp. 12, 2022. 4
- [106] Paul Bergmann, Michael Fauser, David Sattlegger, and Carsten Steger, “Uninformed Students: Student-Teacher Anomaly Detection With Discriminative Latent Embeddings,” in *Proceedings of CVPR*, 2020, pp. 4183–4192. 4
- [107] Hekai Cheng, Lu Yang, and Zulong Liu, “Relation-based knowledge distillation for anomaly detection,” in *Proceedings of PRCV*, 2021, pp. 105–116. 4
- [108] Hanqiu Deng and Xingyu Li, “Anomaly detection via reverse distillation from one-class embedding,” in *Proceedings of CVPR*, 2022, pp. 9737–9746. 4
- [109] Mohammadreza Salehi, Niousha Sadjadi, Soroosh Baselizadeh, Mohammad H. Rohban, and Hamid R. Rabiee, “Multiresolution Knowledge Distillation for Anomaly Detection,” in *Proceedings of CVPR*, 2021, pp. 14902–14912. 4
- [110] Xusheng Wang, Mingtao Pei, and Zhengang Nie, “Self-trained video anomaly detection based on teacher-student model,” in *Proceedings of MLSP*, 2021, pp. 1–6. 4
- [111] Vinod Nair and Geoffrey E Hinton, “Rectified Linear Units Improve Restricted Boltzmann Machines,” in *Proceedings of ICML*, 2010, pp. 807–814. 5
- [112] Ian Goodfellow, Jean Pouget-Abadie, Mehdi Mirza, Bing Xu, David Warde-Farley, Sherjil Ozair, Aaron Courville, and Yoshua Bengio, “Generative adversarial nets,” in *Proceedings of NIPS*, 2014, pp. 2672–2680. 6
- [113] Joseph Redmon and Ali Farhadi, “YOLOv3: An incremental improvement,” *arXiv preprint arXiv:1804.02767*, 2018. 6, 19
- [114] Waqas Sultani, Chen Chen, and Mubarak Shah, “Real-World Anomaly Detection in Surveillance Videos,” in *Proceedings of CVPR*, 2018, pp. 6479–6488. 6, 7
- [115] Jhih-Ciang Wu, He-Yen Hsieh, Ding-Jie Chen, Chiou-Shann Fuh, and Tyng-Luh Liu, “Self-supervised sparse representation for video anomaly detection,” in *Proceedings of ECCV*, 2022, pp. 729–745. 6, 7
- [116] Diederik P. Kingma and Jimmy Ba, “Adam: A method for stochastic optimization,” in *Proceedings of ICLR*, 2015. 7
- [117] Lior Rokach, “Ensemble-based classifiers,” *Artificial Intelligence Review*, vol. 33, pp. 1–39, 2010. 16

Table 2. Micro and macro AUC scores (in %) and FPS rates on the Avenue data set [40], while varying the number of transformer blocks m and the number heads s inside our architecture.

m	s	AUC		FPS
		Micro	Macro	
3	5	67.9	72.2	2266
4	5	72.1	76.7	1806
5	5	75.4	75.5	1480
6	5	68.6	77.4	1256
7	5	72.6	71.9	1100
5	3	70.6	73.3	1476
5	4	74.3	72.9	1487
5	5	75.4	75.5	1480
5	6	68.5	70.6	1472
5	7	72.5	74.6	1460

6. Supplementary

In the supplementary, we present several ablation studies to justify our design choices related to the architecture, the number and resolution of output heads, the number of input frames, the losses, the teachers, and the integration of adversarial training with multiple teachers. Furthermore, we present additional qualitative results.

6.1. Ablation Studies

We start developing our model from a truncated architecture that takes a single frame as input and produces anomaly maps of 4×4 pixels. The truncated architecture is trained using only standard knowledge distillation from a single teacher, namely T_1 [5].

We report both micro and macro AUC scores for our ablation studies. When making our design choices, we refer to the micro AUC as the more representative measure, due to its wider popularity (in contrast to the macro AUC) across video anomaly detection papers.

Transformer architecture. To determine the optimal depth for our convolutional transformer, we first fix the number of heads to $s = 5$ and experiment with architectures comprising m blocks, where $m \in \{3, 4, 5, 6, 7\}$. The results reported in Table 2 indicate that using $m = 5$ transformer blocks leads to the highest micro AUC score, while keeping an astonishing FPS rate of 1480. Next, we fix the number of blocks to $m = 5$ and vary the number of heads, considering $s \in \{3, 4, 5, 6, 7\}$. Unlike the number of blocks, we observe that the number of heads does not have a high impact on the running time. We obtain the highest micro AUC with $s = 5$ heads. We underline that all configurations are much faster than competing anomaly detection methods. We hereby focus on choosing the configuration providing the highest micro AUC for the subsequent experiments, namely the one with $m = 5$ blocks and $s = 5$ heads.

Output heads. The task of replicating the full-resolution

Table 3. Micro and macro AUC scores (in %) on the Avenue data set [40], while varying the resolution and the number of output heads. The top scores are highlighted in bold.

#Output Heads	Head Resolution	AUC	
		Micro	Macro
1	1×1	68.2	74.3
1	4×4	75.4	75.5
1	16×16	65.7	74.0
1	64×64	62.3	65.8
1	Full	59.2	73.9
2	$1 \times 1, 4 \times 4$	71.7	74.7
3	$1 \times 1, 4 \times 4, 16 \times 16$	76.4	76.0

Table 4. Micro and macro AUC scores (in %) on the Avenue data set [40], while varying the number of input frames. The top scores are highlighted in bold.

#Input Frames	AUC	
	Micro	Macro
1	76.4	76.0
3	79.5	80.7
5	78.4	80.3

anomaly maps produced by the state-of-the-art teacher models [4, 5] is quite difficult, and the anomaly detection performance is directly impacted by the ability of the student to replicate the teachers. To simplify the task, we reduce the resolution of the anomaly maps. To determine the optimal resolution, we test different output head configurations, reporting the results in Table 3. According to the presented results, our model seems to achieve better micro AUC scores when producing anomaly maps of 1×1 and 4×4 pixels. The micro AUC tends to drop as we increase the resolution of the anomaly maps. Aside from testing individual output heads, we also consider combining the low-resolution heads into a single architecture with multi-resolution outputs. This approach proves to be useful when combining the 1×1 , 4×4 and 16×16 output heads. We continue our experiments with the architecture comprising these multi-resolution output heads.

Input frames. Many state-of-the-art models for anomaly detection in video, including our teachers [4, 5], introduce temporal information as input to gain performance. Inspired by such methods, we explore the impact of using a temporal sequence of frames as input and present the results in Table 4. We observe that the performance increases by 2-4% for both AUC measures when using 3 video frames as input instead of a single frame. Going up to 5 frames as input does not seem to be further useful. To this end, we opt for providing 3 frames as input for the subsequent experiments.

Losses. Another aspect worth studying is the proposed training procedure, which comprises two phases and three losses. In the first phase, we train the model to reconstruct the middle input frame, optimizing it with the loss \mathcal{L}_{AE} defined in

Table 5. Micro and macro AUC scores (in %) on the Avenue data set [40], while using different training procedures based on input reconstruction pre-training (\mathcal{L}_{AE}), knowledge distillation (\mathcal{L}_{KD}), and adversarial knowledge distillation (\mathcal{L}_{AKD}). The top scores are highlighted in bold.

\mathcal{L}_{AE}	\mathcal{L}_{KD}	\mathcal{L}_{AKD}	AUC	
			Micro	Macro
✓			72.6	73.2
	✓		79.5	80.7
		✓	63.7	69.8
✓	✓		85.0	86.5
✓		✓	69.1	80.6
	✓	✓	82.4	82.9
✓	✓	✓	86.2	86.7

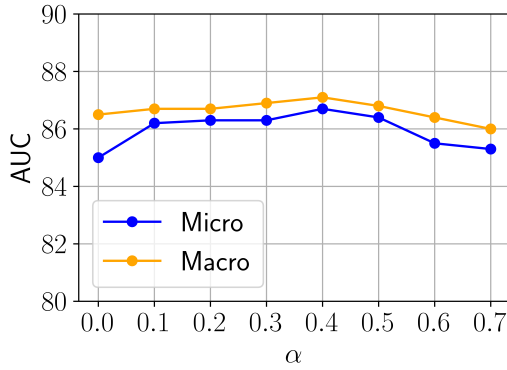


Figure 8. Micro and macro AUC scores (in %) on the Avenue data set [40] for distinct values of the adversarial knowledge distillation weight factor α .

Eq. (2). In the second training phase, the model learns to distill knowledge from one or more teachers, optimizing the joint loss given by the sum of \mathcal{L}_{KD} and \mathcal{L}_{AKD} , as defined in Eq. (7). We study the effect of these three losses, reporting the corresponding results in Table 5. First, we observe that training our model to reconstruct the middle frame is not sufficient to obtain competitive results on Avenue. Standard knowledge distillation obtains significantly better results than middle frame prediction and adversarial distillation. Combining the losses two by two brings improvements over each and every individual counterpart. Nevertheless, the results show that combining all three losses, as proposed in the main article, represents the training procedure achieving the best performance. This confirms that our training strategy is effective.

Adversarial loss weight. Throughout all the experiments involving adversarial knowledge distillation, the hyperparameter controlling the importance of the adversarial distillation loss in Eq. (7) is set to $\alpha = 0.1$. However, to determine if the proposed loss is robust to variations of α , in Figure 8, we present additional results with values of α between 0.1 and 0.7, taken at a step of 0.1. The results for $\alpha = 0$ correspond to the model trained without adversarial knowledge

Table 6. Micro and macro AUC scores (in %) on the Avenue data set [40], while alternating between individual and combined teachers. Results for different attempts of performing adversarial distillation with multiple teachers are also reported. The top scores are highlighted in bold.

Teacher	#Adversarial Discriminators	#Output Branches	AUC	
			Micro	Macro
T_1 [5]	0	1	86.2	86.7
T_2 [4]	0	1	82.1	85.5
T_1 [5] + T_2 [4]	0	1	88.2	87.7
T_1 [5] + T_2 [4]	1	1	85.4	85.7
T_1 [5] + T_2 [4]	2	1	88.0	87.3
T_1 [5] + T_2 [4]	2	2	85.7	85.6

distillation. As indicated by the results illustrated in Figure 8, there are multiple values for α , between 0.1 and 0.5, leading to superior results compared to the baseline based only on standard knowledge distillation (which uses $\alpha = 0$). We thus conclude that the loss proposed in Eq. (7) is robust to variations of α , allowing us to set this hyperparameter without tuning.

Multiple teachers and adversarial training. The ablation results presented so far distill knowledge from a single teacher, namely T_1 [5]. Since different models can often produce distinct anomaly maps, it can be reasonably argued that combining the respective models can lead to performance improvements, an argument which forms the basis of ensemble learning [117]. We conjecture that the same principle applies to knowledge distillation, *i.e.* distilling knowledge from multiple teachers is likely to bring performance gains. To this end, we propose to distill knowledge from two powerful teachers, denoted as T_1 [5] and T_2 [4]. In Table 6, we present results for alternating between individual and combined teachers, applying standard knowledge distillation at first. Our empirical results confirm that introducing two teachers leads to superior micro and macro AUC scores.

We next turn our attention to introducing adversarial knowledge distillation with multiple teachers, which is not trivial. We study three possible ways of integrating multiple teachers with adversarial distillation:

- **One adversarial discriminator, one output branch.** In this configuration, the student has a single multi-resolution output branch for both teachers, and the adversarial discriminator distinguishes between three categories of anomaly maps produced by the student, the teacher T_1 , and the teacher T_2 , respectively. Within this framework, adding more teachers is just a matter of adding more classes to the discriminator.
- **Two adversarial discriminators, one output branch.** In this configuration, the student has a single multi-resolution output branch for both teachers. For each teacher T_i , there is a distinct binary discriminator that classifies the anomaly maps into two classes, one for

Table 7. Micro and macro AUC scores (in %) on Avenue [40], ShanghaiTech [41] and UCSD Ped2 [42], for student models trained with two teachers, before and after adding adversarial distillation. The top scores are highlighted in bold.

Teachers	\mathcal{L}_{AKD}	AUC					
		Avenue		Shanghai		Ped2	
		Micro	Macro	Micro	Macro	Micro	Macro
T_1 [5] + T_2 [4]		88.2	87.7	77.8	84.6	91.7	96.5
T_1 [5] + T_2 [4]	✓	88.0	87.3	77.9	86.0	93.6	97.0

Table 8. Micro and macro AUC scores (in %) and FPS rates on the Avenue data set [40], while alternating between CvT blocks with fully connected (fc) layers (standard) or pointwise convolutions (proposed). The top scores are highlighted in bold.

Architecture	AUC		FPS
	Micro	Macro	
CNN+CvT (standard, with fc)	71.8	77.1	1267
CNN+CvT (pointwise conv, no fc)	85.0	86.5	1480

the student and one for the teacher T_i . Within this framework, adding more teachers requires adding an equal number of adversarial discriminators.

- **Two adversarial discriminators, two output branches.** In this framework, the student has a separate multi-resolution output branch and an associated adversarial discriminator for each teacher T_i . Since there are multiple output branches for this framework, we need a method to aggregate the anomaly maps at a certain resolution. We consider taking the element-wise maximum or the average of the corresponding anomaly maps, reporting the results with the better aggregation function only, namely the element-wise maximum.

In the second part of Table 6, we present the results with the aforementioned frameworks for integrating multiple teachers with adversarial distillation. Among the three alternative frameworks, the best results are obtained by the approach comprising two adversarial discriminators and one output branch. However, it appears that none of the proposed frameworks is able to surpass the results obtained by distilling both teachers with standard knowledge distillation. This seems to contradict our results with a single teacher reported in Table 5, where adversarial knowledge distillation showed promising improvements. To obtain a more reliable assessment of the effect of adding adversarial distillation when using multiple teachers, we extend our comparative study to the ShanghaiTech [41] and UCSD Ped2 [42] data sets. We report the corresponding results in Table 7. The empirical results on the additional data sets refute our initial assessment observed on Avenue. Judging by the extended empirical evaluation on all three data sets, we conclude that adversarial knowledge distillation is useful after all.

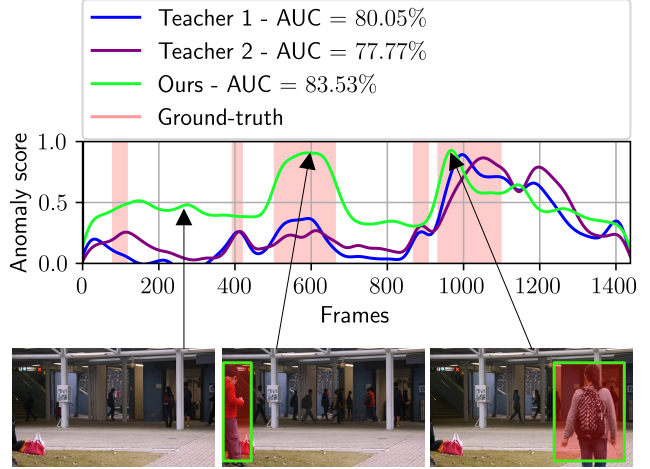


Figure 9. Comparing the frame-level anomaly scores of teachers T_1 [5] and T_2 [4] with the scores of our student on test video 1 from Avenue. The anomaly localization examples are provided by the head with the highest resolution of our student. Best viewed in color.

Dense layers versus pointwise convolutions. In Table 8, we demonstrate the effectiveness of replacing the last two fully connected layers from the CvT block [88] with pointwise convolutions. For a fair comparison, both model variants are trained with middle frame reconstruction in the first training stage and standard knowledge distillation in the second stage. Aside from the expected speed improvement, we observe that the proposed change also generates significantly better micro and macro AUC scores. In conclusion, the empirical evaluation clearly indicates that replacing fully connected layers with pointwise convolutions is beneficial in terms of both speed and accuracy.

6.2. Qualitative Analysis

Frame-level scores. In addition to the figures illustrating examples of frame-level anomaly detection scores included in the main paper, we provide more frame-level output visualizations on three test videos. In Figure 9, we present the anomaly detection performance on test video 1 from Avenue. On this video, our student is remarkably able to surpass both teachers by more than 3% in terms of the AUC. This highlights that, even if the complexity of the student network is significantly lower compared with the complexity of the teachers, the student is able to learn aggregated information, which can eventually lead to surpassing the teachers. An even higher gap in favor of our student is illustrated in Figure 11. Indeed, the frame-level anomaly predictions on test video 01_0136 from ShanghaiTech indicate that our student surpasses the best teacher, T_1 [5], by more than 12%, attaining an overall AUC of 97.46%. For the UCSD Ped2 data set, we showcase the frame-level scores on test video 3 in Figure 12. In this example, the student model attains an AUC score of 98.63%, being very close to the teachers,



Figure 10. Examples of anomaly maps of 16×16 pixels generated by our student and the two teachers, for a set of five randomly chosen test frames from Avenue. For reference, the ground-truth anomaly maps from Avenue are also included. Best viewed in color.

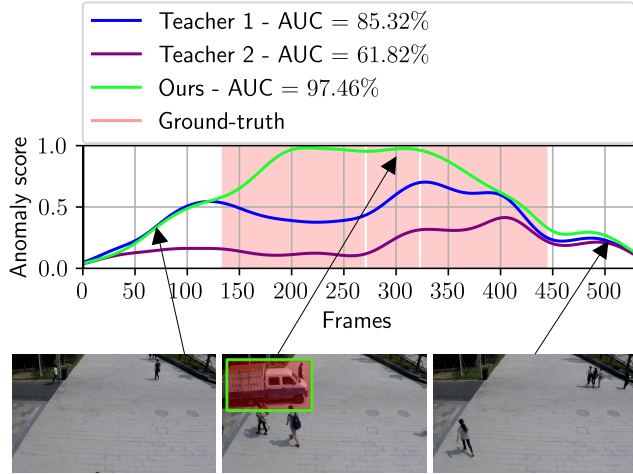


Figure 11. Comparing the frame-level anomaly scores of teachers T_1 [5] and T_2 [4] with the scores of our student on test video 01_0136 from ShanghaiTech. The anomaly localization examples are provided by the head with the highest resolution of our student. Best viewed in color.

which have perfect scores.

Anomaly maps. In Figure 10, we illustrate a set of predicted versus ground-truth anomaly maps for five test frames from Avenue. The anomaly maps on the third row are predicted by our student model, while those on the fourth and fifth

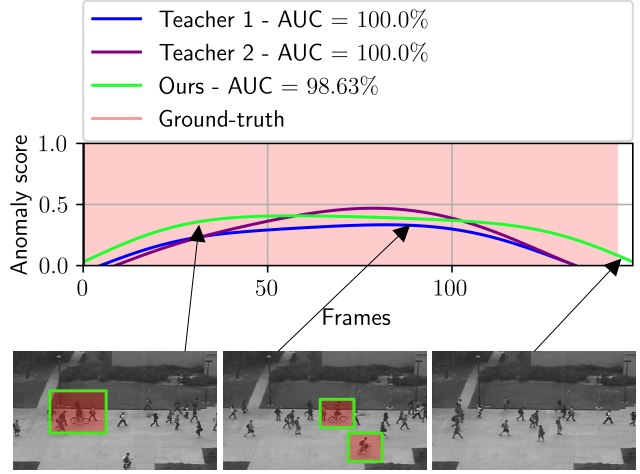


Figure 12. Comparing the frame-level anomaly scores of teachers T_1 [5] and T_2 [4] with the scores of our student on test video 3 from UCSD Ped 2. The anomaly localization examples are provided by the head with the highest resolution of our student. Best viewed in color.

rows are predicted by the teachers T_1 and T_2 , respectively. We underline that the anomaly maps generated by the student are smoother, because it does not rely on a pre-trained detector to obtain object bounding boxes. This feature seems to be extremely helpful for the example depicted on the

second column, where the teachers fail to detect the papers thrown in the air, since *paper* is not among the classes known by YOLOv3 [113]. In contrast, our student assigns high anomaly scores to the region where there are papers in the air. Another interesting behavior for our student is its ability to assign a high score to the child running in the example shown on the fourth column, without triggering high anomaly scores for the person standing on the grass, as opposed to the teachers. The example shown on the last column depicts a normal event, where people are just walking. Here, we observe that teacher T_2 outputs high anomaly scores without reason. In the end, we believe that the most remarkable ability of our student is to detect anomalies where object detectors with a limited number of known classes fail.